Oil & Gas Science and Technology - Rev. IFP Energies nouvelles **74**, 8 (2019)

https://doi.org/10.2516/ogst/2018083

Available online at:
ogst.ifpenergiesnouvelles.fr

REGULAR ARTICLE OPEN ACCESS

Development of fly ash reinforced nanocomposite preformed particle gel for the control of excessive water production in the mature oil fields

Abhinav Kumar[1], Vikas Mahto[2,*], and Virender Parkash Sharma[3]

[1] Senior Research Fellow, Department of Petroleum Engineering, Indian Institute of Technology (Indian School of Mines) Dhanbad, Jharkhand 826004, India
[2] Associate Professor, Department of Petroleum Engineering, Indian Institute of Technology (Indian School of Mines) Dhanbad, Jharkhand 826004, India
[3] Professor, Department of Petroleum Engineering, Indian Institute of Technology (Indian School of Mines) Dhanbad, Jharkhand 826004, India

Received: 7 March 2018 / Accepted: 30 October 2018

Abstract. One of the appropriate methods to minimize water production and increase sweep efficiency is the utilization of Preformed Particle Gel (PPG) in the mature oil fields. In this paper, a new fly ash reinforced nanocomposite PPG was developed by the reaction of acrylamide as monomer, N,N′-Methylenebis (acrylamide) as crosslinker and nano fly ash in presence of Potassium Persulfate as initiator and it was compared with a conventional PPG which was designed without nano fly ash. On the incorporation of nano fly ash, swelling performance and thermal stability of PPG had increased significantly. Rheological data revealed that dynamic moduli (G' and G'') of fly ash reinforced nanocomposite PPG has improved viscoelastic properties with a higher value of critical shear stress as compared to conventional PPG. The single sandpack flow experiment has shown the injectivity of nanocomposite PPG into the sandpack with a maximum resistance factor of 60.57. However, parallel-sandpack flow experiment showed that the newly developed nano fly ash reinforced nanocomposite PPG has a profile improvement rate of 92.98% and 97.83% for the permeability contrast of 2.16 and 4.14 respectively and hence it may be a promising agent in reducing excessive water production in mature oil fields.

1 Introduction

Excessive water production is causing a severe problem in mature oil fields throughout the world (Goudarzi *et al.*, 2015; Imqam and Bai, 2015). This water consists of connate water and the water that has been injected into the formation for the purpose of pressure maintenance inside the reservoirs. Excess water production causes an extra load on the fluid handling facilities, damage due to higher rate of corrosion, problems of scale deposition and shorter economic life of well that still contain a significant volume of hydrocarbons (Bai *et al.*, 2007b; Liu *et al.*, 2006). Additionally, environmental problems also arise concerning the disposal of the excess produced water (Simjoo *et al.*, 2009). Therefore, it has become a necessity for the oil industry to find cost-effective ways for handling relatively large amount of water in an environmentally accepted manner.

Globally, on an average of three barrels of water is being produced with every barrel of oil (Crabtree *et al.*, 2000). The main reason behind the production of the huge amount of water is reservoir heterogeneity which severely affects the flow of reservoir fluids (Bai *et al.*, 2008, 2012). Many reservoirs have been hydraulically fractured (either intentionally or unintentionally) or developed large channels due to both mineral dissolution and production during water flooding and these fractured networks or developed large channels are the causes of water production from such reservoirs.

There are various techniques which are available for controlling excessive water production. Customarily, *in situ* bulk gels are being used for conformance control. They consist of a mixture of polymer and crosslinker, called gelant, is injected to target formation either together or separately with a slug. A crosslinking reaction then occurs by using a specific trigger to generate *in-situ* gels at reservoir temperature which reduce the reservoir heterogeneity (Al-Muntasheri *et al.*, 2009, 2006; Chauveteau *et al.*, 1999). Although, polymer gels are the most efficient, cost-effective means for decreasing water production and improving reservoir homogeneity in mature oil fields (Seright and Liang, 1994), this technology, however, has several

* Corresponding author: vikas.ismpe@hotmail.com

disadvantages that restrict its applications for conventional reservoirs, such as a lack of gelation time control, gelling uncertainty due to shear degradation, chromatographic separation between polymer and crosslinker, and dilution by the formation of water and minerals (Bai *et al.*, 2008; Chauveteau *et al.*, 2003; Coste *et al.*, 2000).

In last few decades, *in-situ* gels had been widely used in mature oil field for conformance control in which a mixture of polymer and crosslinker, called gelant, is injected into the concerned mature formation. It reacts at reservoir temperature to form a gel which seals the formation either fully or partially. A recent advancement in gel treatment method uses Preformed Particle Gel (PPG) to overcome the limitation of *in-situ* gels (Bai *et al.*, 2007b). PPGs are formed at surface facilities which removes the concept of gelation in reservoir completely. PPGs requires less equipment for the preparation at the surface. However, gel particles may vary from nanometre range to a few millimetres (Bai *et al.*, 2007a, 2008).

The mechanism of gel extrusion through fractures largely depends on gel composition, gel volume, and optimum gel placement (Seright, 1999). During extrusion of gel through fractures, gel moved as a plug and that negligible viscous dissipation occurred during the gel plug movement (Seright, 1999, 2000). A series of Core flooding experiments demonstrate that the flow of gel is seized as soon as gelation occurs (Seright, 1995). The preformed gels have better efficiency in reducing water flow through fractures compared to *in-situ* gels without inducing substantial formation damage and impose less damage in low permeable oil zones (Seright, 1995, 1999). The flow and transport of microgels through sandpack depicts that microgels are a good candidate for water shutoff and profile modification without any problem of plugging (Feng *et al.*, 2003; Rousseau *et al.*, 2005).

However, despite the various benefits of preformed gels over *in-situ* gels, until now preformed gels have not shown a very effective solution to the problem of conformance control and reservoir heterogeneity. Some of the limitations of preformed gels include (a) swelling: inadequate swelling ability, (b) elasticity: inadequate gel elasticity, (c) mechanical: low strength and toughness, and (d) thermal: insufficient thermal resistance to withstand very extreme reservoir conditions, shorter degradation time (Tongwa and Baojun, 2015). To overcome these limitations nanomaterial may be incorporated into the conventional PPG.

In this research work, a fly ash reinforced nanocomposite PPG was developed and compared with conventional PPG. It has better thermal stability and adequate mechanical strength and toughness and improved performance in controlling excessive water production from the heterogeneous reservoirs.

2 Experiment

2.1 Materials

Acrylamide, AM (Assay (GC, area%) $\geq$ 99%) was purchased from *Merck Chemicals, Germany*, which is white granular and completely soluble in water. N,N′-Methylenebis (acrylamide), used as a crosslinker, was purchased from *Sigma-Aldrich*. Nano fly ash used in this extensive study was purchased from *Intelligent Materials Pvt. Ltd., India*. Polymerization of the monomer of acrylamide solution was initiated by Potassium persulfate ($K_2S_2O_8$, KPS) used as a redox initiator in this case and were purchased from *Sigma Aldrich*. Sodium Chloride, NaCl (99.8%) was purchased from Finar Reagent and used as received. Distilled water was used for the synthesis while 20 000 mg/L brine solution was used for all the experiments.

2.2 Performed particle gel preparation

First of all, 20 g of acrylamide was dissolved in 100 mL of distilled water in a beaker. The mixture was stirred for 10 min. Then 0.2% (0.2 g) of nano fly ash, which is in very fine powder form, was added to the solution. Homogenization was immediately performed on the solution of nano fly ash and acrylamide by an Ultrasonic Homogenizer (TAKASHI Model: U250) for half an hour in order to restrict the formation of a lump of fly ash. To ensure complete exfoliation of fly ash nanomaterial the solution of nano fly ash and acrylamide, after homogenization, was stirred vigorously for about 24 h. Afterwards, 300 ppm of N,N′-Methylenebis (acrylamide), used as a crosslinker, was added to the solution and stirred for another 10 min. Subsequently, the solution was poured in three-necked round bottom flask equipped with an inlet and outlet tubes for nitrogen gas. The obtained solution in three-necked round bottom flask was then kept in an oil bath at 40 °C and purged with nitrogen gas for 30 min before 100 ppm of KPS was added to the solution. This resulting solution was then kept at 40 °C for 10–12 h to make sure for complete gelation to occur. The strong and elastic bulk gel was formed and was cut into pieces. The reaction mechanism of fly ash reinforced nanocomposite is illustrated in Figure 1. It was then cleansed by soaking in a large amount of distilled water for 3–4 days to wash out unreacted monomers, followed by drying in an oven at 60 °C until the change in weight is zero. The dried gel was crushed into small particle sizes by Blending Machine, called Preformed Particle Gel (PPG). The crushed PPG particles with a particle size between 40 and 50 meshes were selected for characterization and evaluation of PPG properties. However, aforementioned particles size of PPG could be obtained by sieving experiment using standard ASTM sieve size of 40 and 50 *i.e.*, PPG particles that pass-through ASTM 40 mesh size and could not pass-through ASTM 50 size will have a size between 40 and 50 meshes. The identical procedure was followed for preparing gels with no nanomaterial *i.e.* with no nano fly.

2.3 Characterization

Dynamic Light Scattering (DLS), sometimes termed as Quasi-Elastic Light Scattering (QELS) techniques were used to determine particle size distributions of nano fly ash which is carried out by Zetasizer Nano-S90 (*Malvern Instrument Ltd., UK*) at the room temperature. In order to understand the effects of particle sizes on the crystallization of nano fly ash Powder X-Ray Diffraction (PXRD) were analysed by Model D8 advance (*Bruker, Billerica, MA, USA*). For evaluating thermal degradability of the swollen PPG and

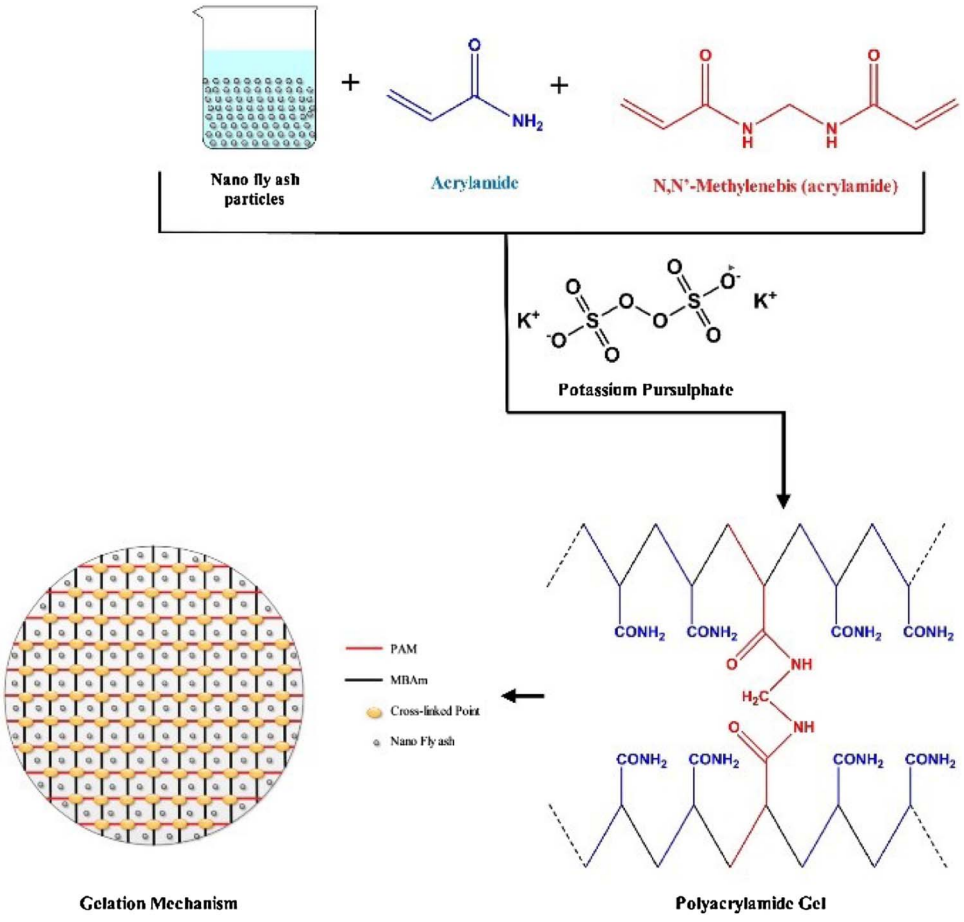

Fig. 1. A typical gelation of fly ash reinforced nanocomposite gel.

nanocomposite PPG Thermogravimetric Analysis (TGA) was conducted by using TGA7 (*PerkinElmer, Waltham, MA, USA*). The Field Emission Scanning Electron Microscope (FESEM) was carried out to delineate surface morphology of the obtained PPG with and without nano fly ash on FE-SEM Supra 55 with Air Lock chamber (*Carl Zeiss, Oberkochen, Germany*). Energy-dispersive X-ray spectroscopy (EDX) was performed to depict the elemental composition of nano fly ash along with obtained PPG using an extension of the aforementioned FE-SEM equipment.

2.4 Methods

The following properties were evaluated for the nanocomposite PPG.

2.4.1 Swelling kinetics

The evaluation of swelling kinetics of PPG is prerequisite to determine its ability to swell and plug the reservoir high permeable streaks and fractures. The swelling ratio is the mass ratio of the PPG before and after swelling (Bai *et al.*, 2012). The swelling ratio of the PPG was evaluated three times on identical samples in 20 000 ppm of brine solution at 70 °C from the following equation (1):

$$\text{Swelling ratio} = \frac{W_s - W_d}{W_d}, \quad (1)$$

where, W_s = weight of swollen of PPG, W_d = weight of dry PPG.

2.4.2 Rheological measurements

Measurement of PPG rheology was performed on Oscillatory Viscometer: Bohlin Gemini II Rheometer (*Malvern Instruments, Malvern, UK*) with parallel plate measuring system for determining the viscoelastic behaviour. The amplitude sweep test of PPG pack was conducted within the stress range of 1–2000 Pa at a fixed frequency of 0.1 Hz. Subsequently, the frequency sweep measurements were performed at a frequency in the range of 0.01–10.00 Hz, in the oscillation mode at a strain rate of 0.005 s^{-1}.

2.5 Sandpack experiment

2.5.1 Single sandpack experiment

Single sandpack experiment was carried out to evaluate the injectivity of the particles of obtained fly ash reinforced nanocomposite PPG. The sandpack (length = 15 cm and diameter = 3 cm) was used to simulate the particle-fluid flow. The size of the particle used for the sandpack flooding

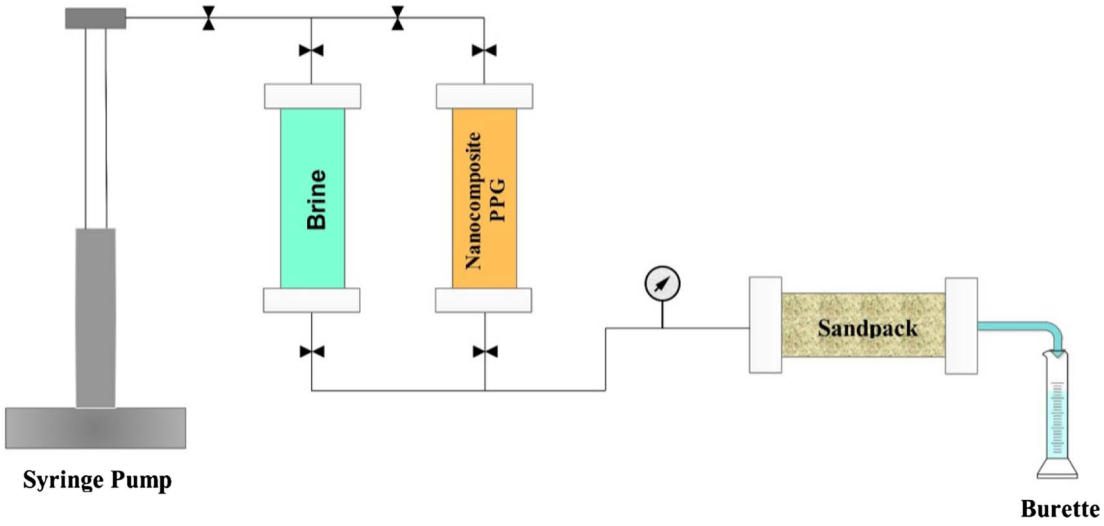

Fig. 2. Schematic diagram of single sandpack experimental setup.

ranges between different mesh sizes from 20 to 40 meshes with a concentration of 2% by weight in the brine solution. The schematic diagram of the used experimental setup has been illustrated in Figure 2.

The Resistance factor (R_F) was determined by the following formula (2):

$$R_F = \frac{\lambda_w}{\lambda_{ppg}} = \frac{K_w/\mu_w}{K_{ppg}/\mu_{ppg}}, \quad (2)$$

where λ_w = mobility of the brine solution, λ_{ppg} = mobility of the PPG solution, K_w = sandpack permeability with brine flooding, μ_w = viscosity of the brine solution, K_{ppg} = sandpack permeability with PPG solution flooding, μ_{ppg} = viscosity of the PPG solution.

According to the Darcy law, the sandpack permeability K (K_w; K_{ppg}) can be evaluated using the following formula (3):

$$K = \frac{Q\mu L}{A\Delta P}, \quad (3)$$

where Q = the flow rate (cm^3/s), μ = the viscosity of the brine (in cP), L = Length of sandpack (cm), A = cross-sectional area of sandpack (cm^2), ΔP = pressure drop across the sandpack (atm).

Combining equations (2) and (3), we get

$$R_F = \frac{\Delta P_{ppg}}{\Delta P_w}, \quad (4)$$

where ΔP_{ppg} = pressure difference of the injected PPG solution, ΔP_w = pressure difference of the injected brine solution.

2.5.2 Parallel sandpack experiment

The concept behind conducting parallel sandpack experiment is to deduce the capability of the fly ash reinforced nanocomposite PPG particles entering and blocking the sandpack. Two sandpacks of substantial permeability contrast were prepared. The prepared sandpacks, then, assembled in a manner as shown in Figure 3.

In the parallel sandpack experiment, the permeabilities of sandpacks were determined by flooding it with brine solution. Amount of brine produced during brine flooding was recorded from both the sandpack (*i.e.* high permeable and low permeable). After that 1.0 PV nanocomposite PPG suspension is injected into the parallel sandpack with a constant velocity of 5 mL/min. Subsequently, the parallel sandpacks were disassembled and sealed before keeping them into the oven at 70 °C for 24 h–48 h. After completion of ageing in an oven at 70 °C for 24 h–48 h, both sandpacks were reassembled in the experimental apparatus, as shown in Figure 3. Brine was again injected to flood the sandpack until the pressure and produced fluid reached a stable condition. The fluid produced is noted to compute the profile improvement rate according to the following formula (5) were recorded (Zhao *et al.*, 2018):

$$f = \frac{q_{hb}/q_{lb} - q_{ha}/q_{la}}{q_{hb}/q_{lb}}, \quad (5)$$

where f = profile improvement rate, q_{hb} = water produced rate before the PPG-particle injection in high permeable sandpack and q_{lb} = water produced rate before the PPG particle injection in low permeable sandpack, q_{ha} = water produced rate after the PPG particle injection in high permeable sandpack and q_{la} = water produced rate after the PPG-particle injection in low permeable sandpack. The experiment of flooding with brine solution before and after nanocomposite PPG injection has been carried out three times on identical parallel sandpacks.

3 Result and discussion

3.1 Particle size of fly ash

Particle size influences many properties of materials and is an extremely useful indicator of quality and performance.

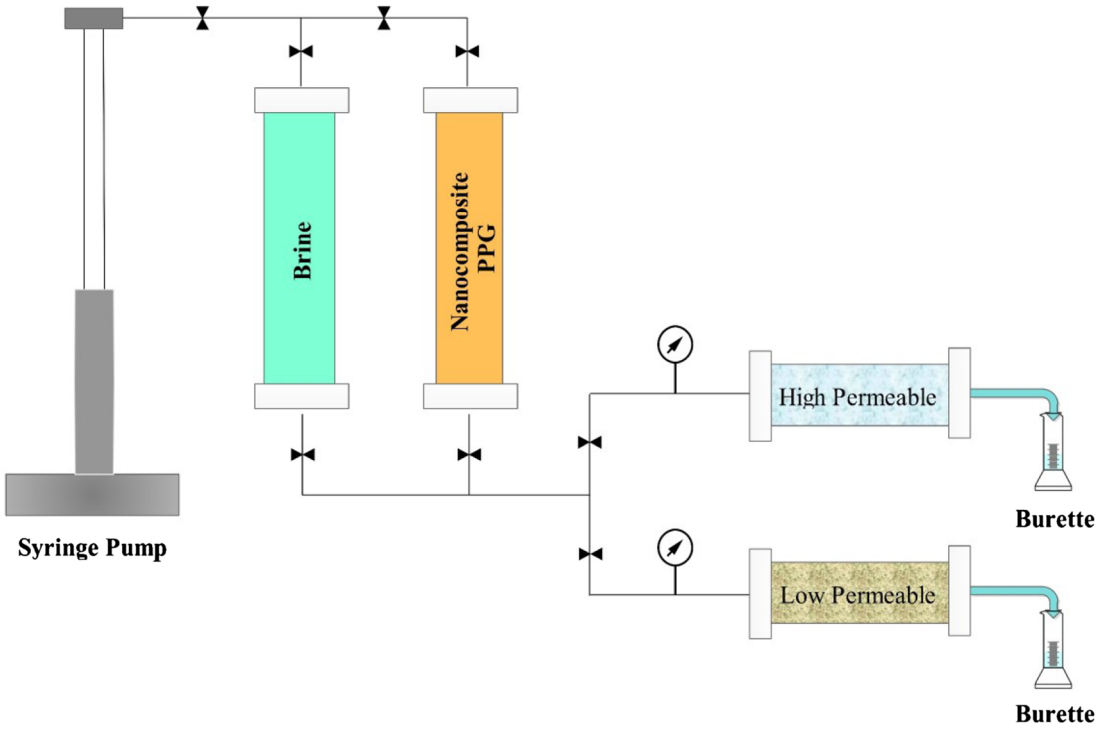

Fig. 3. Schematic diagram of parallel sandpack experimental apparatus.

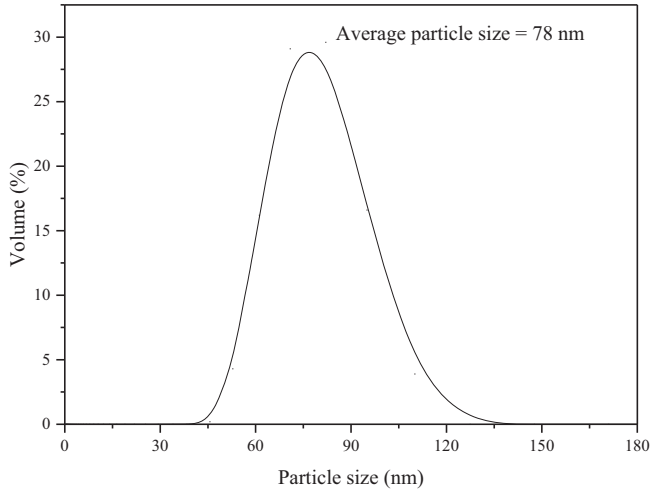

Fig. 4. Particle size distribution of nano fly ash.

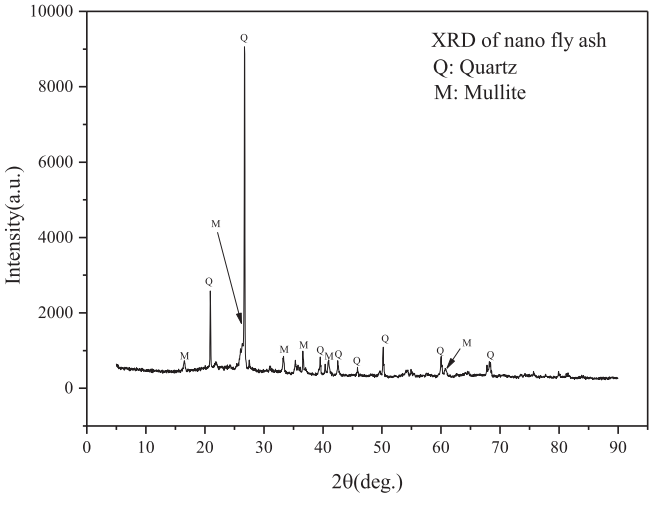

Fig. 5. X-ray diffraction spectra of nano fly ash showing main crystalline phases.

The average particle size of nano fly ash was found to be 78 nm as shown in Figure 4.

3.2 XRD analysis

In order to examine the crystallinity of the nano fly ash X-ray diffraction was conducted from 5 to 90 2θ angle as shown in Figure 5. It can be deduced from the XRD curve that the predominant phases are quartz (SiO_2) with a major peak at 26.9 2θ and mullite ($3Al_2O_3SiO_2$) with major peaks at around 26.4 2θ. As a result of these observations, the impact caused by the addition of nano fly ash was due to two different crystalline ash particle sizes, not on the chemical elements and compositions of the ash.

3.3 TG analysis

For appropriate investigation of the thermal stability of PPG and fly ash reinforced nanocomposite PPG, Thermogravimetric Analysis (TGA) of the swollen (*i.e.* in brine with a concentration of 20 000 ppm) PPG and

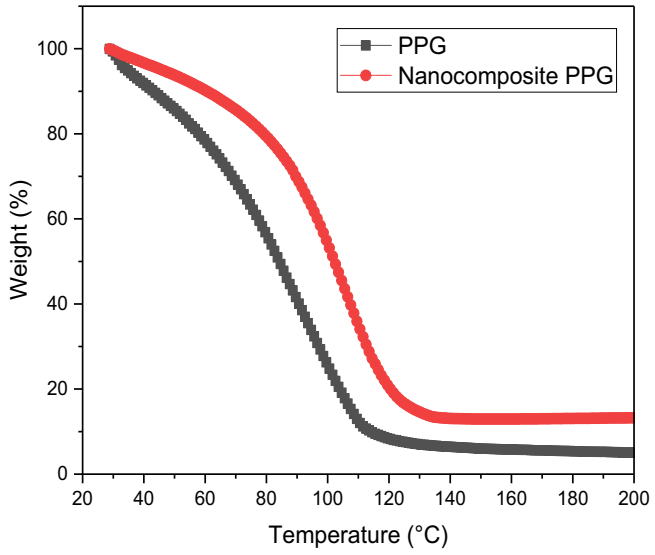

Fig. 6. Thermogravimetric analysis of swollen PPG and nanocomposite PPG.

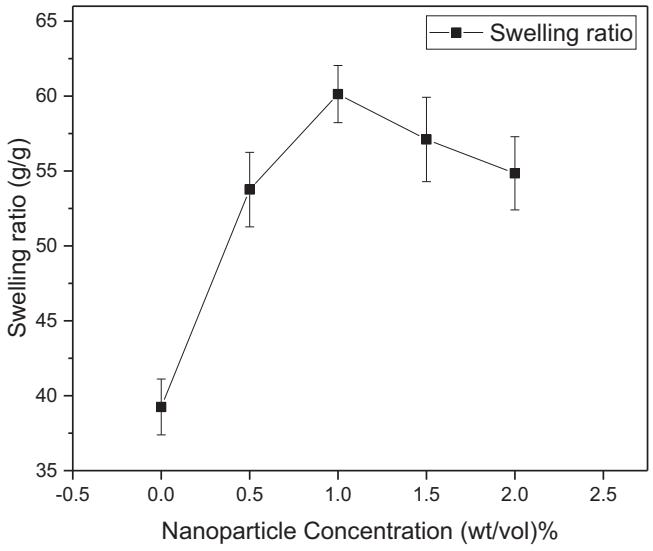

Fig. 7. The swelling ratio of nanocomposite PPG at varying concentration of nano fly ash.

nanocomposite PPG was carried out at a heating rate of 10 °C/min, in nitrogen atmosphere from ambient temperature to 200 °C. The temperature and salinity were taken as a representative of the reservoir. Thermogravimetric analysis profiles of PPG with and without nanomaterial is shown in Figure 6. From the curve, it can be stated that a weight loss of up to 70% and 50% observed between room temperature and 100 °C for PPG and nanocomposite PPG respectively, which corresponds to evaporation of water and continuous vaporization. In the next step, 101–120 °C, weight loss is 22% and 28% for PPG and nanocomposite PPG respectively. This loss may be due to the eradication of water molecules from the two neighbouring carboxyl groups of the polymer chains with the formation of anhydride and chain scission removing CO and CO_2. After 120 °C curve appears to be constant with a total loss of 92% and 78% observed for PPG and nanocomposite PPG respectively. This may conclude a slightly higher thermal stability of nanocomposite PPG in the reservoir.

3.4 Evaluation of swelling kinetics

The swelling ratio of fly ash reinforced nanocomposite PPG at different concentration of nano fly ash is plotted in Figure 7. It can be interpreted from the graph that addition of nano fly ash initially increases up to a maximum value of 52% at 1 (wt/vol) % of nano fly ash and the decreases gradually and become constant afterwards.

3.5 FESEM

SEM and EDAX analysis were performed on nano fly ash and dried PPGs to understand the surface morphology and retained constituents respectively. Figure 8a is showing the general features of the original fly ash. From the figure, it can be seen the fly ash is mostly constituted by compact or hollowed spheres but with a regular smooth texture. On the surface of spheres, the existence of solid deposits or small crystals could be observed which could be particles of quartz and mullite crystals (Fig. 8d). A dense network of polymer gel with refinement in size in nanocomposite PPG (Fig. 8c) as compared to PPG with no nano fly ash (Fig. 8b) may be easily viewed. Moreover, the presence of a few numbers of micropores can be seen in nanocomposite PPG (Fig. 8c) which is absent in conventional PPG Figure 8b. In addition to this, incorporation of Si in nanocomposite PPG (Fig. 8f) and its absence in conventional PPG (Fig. 8e) could be clearly seen.

3.6 Evaluation of rheological properties

The viscoelastic properties of PPG pack were measured in the purposed study. The viscoelasticity of the PPG pack was characterized by evaluating the elastic modulus (G') and the viscous modulus (G'').

The shear modulus can be written in complex form as

$$G^* = G'' + \mathrm{i}G'' = \frac{\tau_o(t)}{\gamma_o(t)}, \tag{6}$$

$$G' = G^* \cos\delta = \frac{\tau_o}{\gamma_o}\cos\delta, \tag{7}$$

$$G'' = G^* \sin\delta = \frac{\tau_o}{\gamma_o}\sin\delta, \tag{8}$$

where G' = elastic modulus or storage modulus (Pa), G'' = viscous modulus or loss modulus (Pa), τ_o = shear stress (Pa), γ_o = shear strain and δ = phase shift angle.

The storage modulus is the measure of the energy stored by the material during cycle of deformation but it can be recoverable afterwards. The loss modulus is the measure of energy dissipated or lost during the shear cycle and is irreversibly lost. In terms of phase shift angle, an in-phase stress to an applied strain is known as "Elastic" and

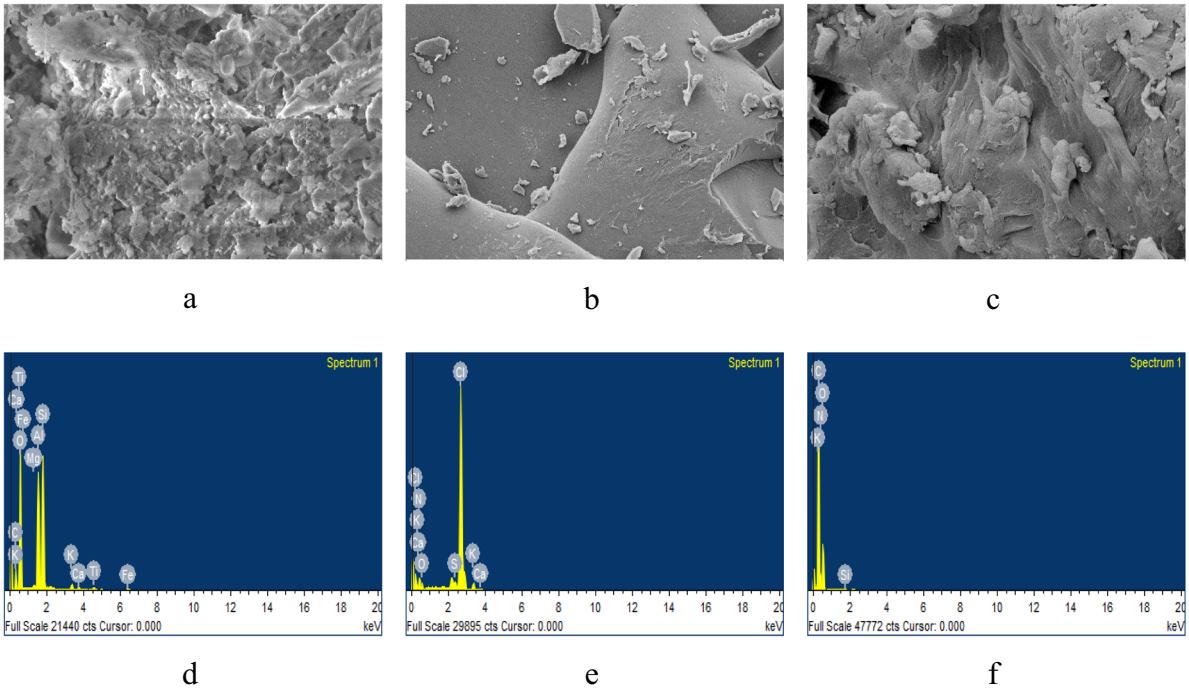

Fig. 8. SEM images of (a) nano fly ash, (b) PPG, (c) nanocomposite PPG and EDAX spectra of (d) nano fly ash (e) PPG (f) nanocomposite PPG.

90° out-of-phase stress response is called "Viscous". Therefore, the term "visco-elastic" is defined for the phase shift angle within $0 < \delta < 90°$. If the substance is purely elastic $\delta = 0$ (*i.e.* $G^* = G'$) and if the substance is purely viscous $\delta = 90°$ (*i.e.* $G^* = G''$).

For the purpose of comparison between PPG pack and fly ash reinforced nanocomposite PPG pack the rheological properties were investigated in the following sections. The linear region was located from the amplitude seep test and it was found to be in the frequency range of 0.01–10 rad s^{-1}.

Stress sweep test was conducted for measuring the resistive ability to shear deformation of PPG and nanocomposite PPG (1% nano fly ash). The results are plotted in Figure 9. It is quite clear from the graph, for fly ash reinforced nanocomposite PPG in the linear viscoelastic region, the value of storage modulus (G') and loss modulus (G'') is higher than that of PPG with no nano fly ash. One more point can be noted from the graph that within the linear viscoelastic region, the elastic modulus (G') predominated over loss modulus (G''), which shows elastic component occupies larger portion of PPG pack. Moreover, the dynamic moduli decrease rapidly as soon as shear stress exceeds τ_c (*i.e.* critical stress value which is the shear resistance of molecular aggregates) and rate of decrement is faster for G' than that of G'' when applied stress crosses the τ_c value indicating viscous behavior is more dominating for higher shear stress. In comparison to PPG with no nano fly ash, nanocomposite PPG exhibits significantly higher τ_c for both the dynamic moduli *i.e.* G' and G''.

Frequency sweep experiments were performed for determining G' and G'' for both PPG with no nano fly ash and

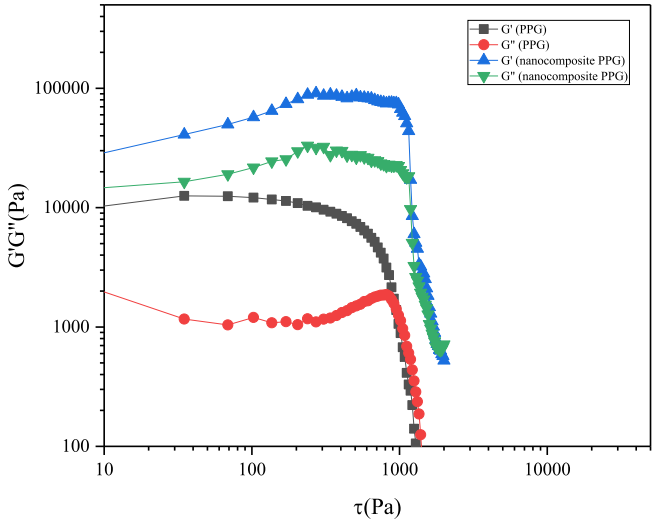

Fig. 9. Dynamic moduli ($G'G''$) as a function of shear stress for PPG and nanocomposite PPG, $f = 0.1$ Hz and $T = 343$ K.

fly ash reinforced nanocomposite PPG. The experimental results are plotted in Figure 10. Value of both the dynamic moduli (*i.e.* G' and G'') are higher in nanocomposite PPG than PPG with no nano fly ash which shows a higher viscoelastic property is incorporated by adding nanomaterial in it. Also, it is clear from the graph that the value of elastic modulus predominates over the loss modulus in the entire frequency range, demonstrating the elastic component dominates the viscous component in the viscoelasticity.

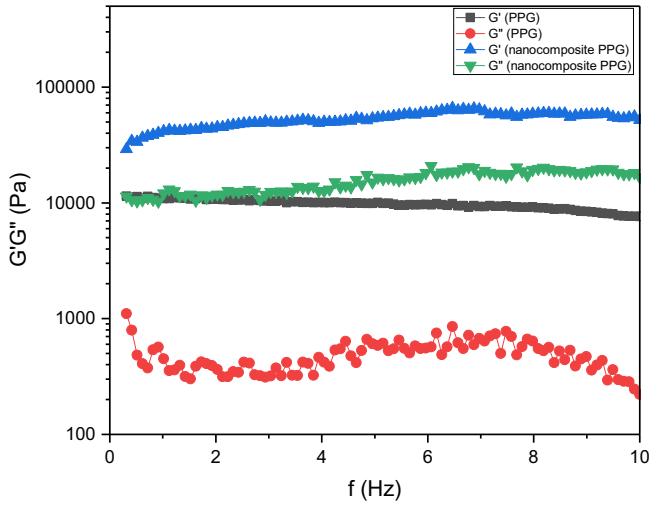

Fig. 10. Dynamic moduli ($G'G''$) as a function of shear frequency for PPG and nanocomposite PPG, $\gamma = 0.005\ s^{-1}$ and $T = 343$ K.

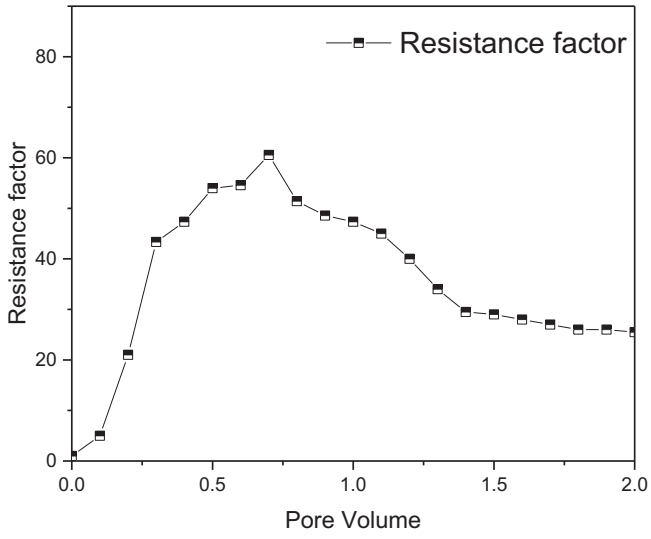

Fig. 11. R_F as a function of pore volume.

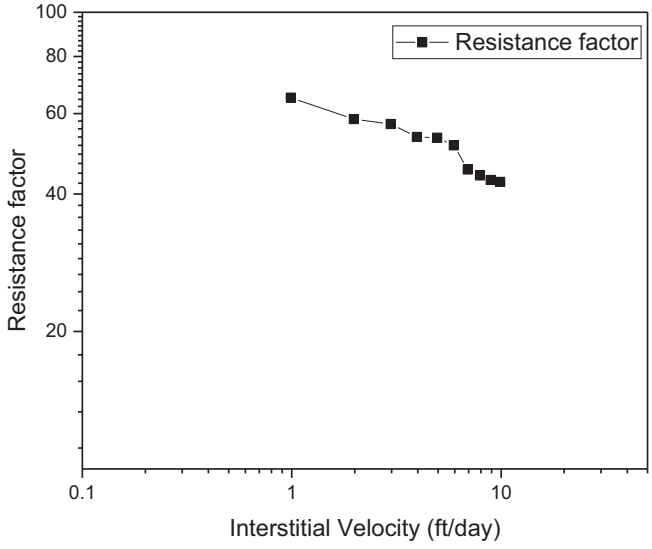

Fig. 12. R_F as a function of interstitial velocity.

The study on rheological properties of fly ash reinforced nanocomposite PPG exhibits more elastic nature of PPG gelled system, which can alter their shape because of the shear force caused by flowing water and the deformed particle can regain its original shape after entering into larger pores. Therefore, a nanocomposite PPG could be a more suitable profile controlling agent due to its significantly higher elastic modulus in comparison to conventional PPG.

3.7 Evaluation of sandpack experiment

3.7.1 Single sandpack experiment

The porosity and permeability were found to be 22.3% and 1.38 Darcy. While injecting fly ash reinforced nanocomposite, PPG Resistance Factor (R_F) as a function of the pore volume injected is plotted in Figure 11. It was noted from the graph that R_F gradually increases attains a maximum value of 60.57 at 0.7 pore volume then decreases gradually and becomes constant at a RF value of 20. The rise in the curve may be due to the critical shear stress (τ_c) of the bigger particles to invade the small pores; once it overcomes the critical shear stress (τ_c) due to the force exerted by the flowing water the curve starts showing a decreasing trend due to the decrease in pressure drop and becomes constant afterwards. Additionally, the effluent that is being collected at the outlet of the sandpack contains PPG particles which may suggest its notable injection and transmission ability.

The Resistance Factor as a function of interstitial velocity has also been plotted by injecting nanocomposite PPG at varying flow rate from 0.5 mL/min (interstitial velocity 0.99 ft/day) to 5 mL/min (interstitial velocity 9.09 ft/day). From Figure 12, it can be inferred that the resistance factor has a decreasing trend with an increase in interstitial velocity. This trend may be interpreted as; the increase in interstitial velocity causes the shear rate to increase and resistance factor to decrease, which in turn gives a typical shear thinning behaviour of nanocomposite PPG solution in the sandpack. This shear thinning behaviour of nanocomposite PPG may result in its better injectivity into the sandpack.

3.7.2 Parallel sandpack experiment

Parallel sandpack flooding experiments were performed in two different sets of sandpacks with similar dimensions but having different permeability contrast (2.16 and 4.14). The outcomes of experiments for improving profile were tabulated in Table 1. It can be clearly deduced from the table that the water produced rate from high permeability streaks (*i.e.* Nos. 1 and 3 sandpacks) were 88% and 91% before nanocomposite PPG particle injection which were reduced to 34% and 18% after particle injection.

Table 1. Profile improvement rate of fly ash reinforced nanocomposite PPG in different sets of sandpack having significant permeability contrast.

Experiment Sets	Sandpack sample	Permeability (μm^2)	Permeability contrast	Ratio of water produced		f (%)
				q_{hb}	q_{ha}	
I	1	2.64	2.16	88/12	34/66	92.98 ± 2.80
	2	1.22				
II	3	5.92	4.14	91/9	18/82	97.83 ± 0.98
	4	1.43				

This clearly points towards the profile control ability of the PPG particles.

In addition, Table 1 also illustrates the better profile control rate for the higher values of permeability contrast. Moreover, more than 92% and 97% profile improvement rate is attained for the permeability contrast of 2.12 and 4.14 respectively using the nanocomposite PPG particle injection.

4 Conclusion

The following conclusions were drawn from the present research studies:

- A fly ash reinforced nanocomposite PPG has been synthesized using nano fly ash and evaluated for conformance control.
- DLS of fly ash sample confirms the size of the fly ash is in nano range *i.e.* <100 nm.
- TG analysis of fly ash reinforced nanocomposite PPG suggests better thermal stability compared to conventional PPG.
- Nanocomposite PPG reflects a better swelling ratio in 20 000 mg/L brine at 70 °C.
- The rheological properties of fly ash reinforced nanocomposite PPG indicate it has higher of value elastic modulus; inferring it to be a better excessive water controlling agent in mature oil fields.
- The single sandpack experiments substantiate nanocomposite PPG has a good injectivity.
- Parallel sandpack tests confirm that fly ash reinforced nanocomposite PPG can significantly create a fluid diversion and cause an increment of swept volume in low permeable sandpack. A high-profile improvement rate of around 93% and 98% have been achieved for a permeability contrast of 2.16 and 4.14 respectively. This results also suggest a notable point *i.e.* as the permeability ratio of the two sandpacks becomes larger the profile improvement rate turns out to be more effective.

References

Al-Muntasheri G.A., Nasr-El-Din H.A., Peters J., Zitha P.L.J. (2006) Investigation of a high temperature organic water shutoff gel: reaction mechanisms, *SPE J.* **11**, 4, 497–504. https://doi.org/ 10.2118/97530-PA.

Al-Muntasheri G.A., Nasr-El-Din H.A., Al-Noaimi K., Zitha P.L.J. (2009) A study of polyacrylamide-based gels cross-linked with polyethyleneimine, *SPE J.* **14**, 2, 245–251. https://doi.org/ 10.2118/105925-PA.

Bai B., Li L., Liu Y., Liu H., Wang Z., You C. (2007a) Preformed particle gel for conformance control: factors affecting its properties and applications, *SPE Reserv. Eval. Eng.* **10**, 4, 415–422. https://doi.org/10.2118/89389-PA.

Bai B., Liu Y., Coste J.-P., Li L. (2007b) Preformed particle gel for conformance control: transport mechanism through porous media, *SPE Reserv. Eval. Eng.* **10**, 2, 176–184. https://doi.org/10.2118/89468-PA.

Bai B., Huang F., Liu Y., Seright R.S., Wang Y. (2008) Case study on preformed particle gel for in-depth fluid diversion, *SPE Symposium on Improved Oil Recovery*, Tulsa, Oklahoma, USA, April 20–23. https://doi.org/10.2118/113997-MS.

Bai B., Wei M., Liu Y. (2012) Injecting large volumes of preformed particle gel for water conformance control, *Oil Gas Sci. Technol. - Rev. IFP Energies nouvelles* **67**, 6, 941–952. doi: 10.2516/ogst/2012058.

Chauveteau G., Tabary R., Renard M., Omari A., Bordeaux U. (1999) Controlling in-situ gelation of polyacrylamides by zirconium for water shutoff, *SPE International Symposium on Oilfield Chemistry held in Houston*, Texas, USA, February 16–19. https://doi.org/10.2118/50752-MS.

Chauveteau G., Tabary R., Le Bon C., Renard M., Feng Y., Omari A. (2003) In-depth permeability control by adsorption of soft size-controlled microgels, *SPE European Formation Damage Conference*, The Hague, Netherlands, May 13–14. https://doi.org/10.2118/82228-MS.

Coste J.P., Liu Y., Bai B., Li Y., Shen P., Wang Z., Zhu G. (2000) In-depth fluid diversion by pre-gelled particles. Laboratory study and Pilot Testing, *SPE/DOE Improved Oil Recovery Symposium*, Tulsa, Oklahoma, April 3–5. https://doi.org/10.2118/59362-MS.

Crabtree M., Romano C., Tyrie J., Elphick J., Kuchuk F., Romano C., Roodhart L. (2000) *Water Control*, Schlumberger, pp. 30–51.

Feng Y., Tabary R., Renard M. (2003) Characteristics of microgels designed for water shutoff and profile control, *SPE International Symposium on Oilfield Chemistry*, Houston, Texas, USA, February 5–7. https://doi.org/10.2118/80203-MS.

Goudarzi A., Zhang H., Varavei A., Taksaudom P., Hu Y., Delshad M., Bai B., Sepehrnoori K. (2015) A laboratory and simulation study of preformed particle gels for water conformance control, *Fuel* **140**, 502–513. https://doi.org/10.1016/j.fuel.2014.09.081.

Imqam A., Bai B. (2015) Optimizing the strength and size of preformed particle gels for better conformance control treatment, *Fuel* **148**, 178–185. https://doi.org/10.1016/j.fuel.2015.01.022.

Liu Y., Zhu M., Liu X., Zhang W., Sun B., Chen Y., Adler H.P. (2006) High clay content nanocomposite hydrogels with surprising mechanical strength and interesting deswelling kinetics, *Polymer*. **47**, 1, 1–5. https://doi.org/10.1016/j.polymer.2005.11.030.

Rousseau D., Chauveteau G., Renard M., Tabary R., Zaitoun A., Mallo P., Braun O., Omari A. (2005) Rheology and transport in porous media of new water shutoff/conformance control microgels, *SPE International Symposium on Oilfield Chemistry*, Houston, USA, February 2–4. https://doi.org/10.2118/93254-MS.

Seright R.S. (1995) Gel placement in fractured systems, *SPE Prod. Facil.* **10**, 4, 241–248. https://doi.org/10.2118/27740-PA.

Seright R.S. (1999) Mechanism for gel propagation through fractures, *SPE Rocky Mountain Regional Meeting*, Gillette, Wyoming, USA, May 15–18. https://doi.org/10.2118/55628-MS.

Seright R.S. (2000) Gel propagation through fractures, *SPE/DOE Improved Oil Recovery Symposium*, Tulsa, Oklahoma, USA, April 3–5. https://doi.org/10.2118/59316-MS.

Seright R.S., Liang J. (1994) A survey of field applications of gel treatments for water shutoff, *Proceedings of SPE Latin America/Caribbean Petroleum Engineering Conference*, Buenos Aires, Argentina, April 27–29. https://doi.org/10.2523/26991-MS.

Simjoo M., Koohi A.D., Seftie M.V., Zitha P.L.J. (2009) Water shut-off in a fractured system using a robust polymer gel, *8th European Formation Damage Conference*, Scheveningen, The Netherlands, May 27–29. https://doi.org/10.2118/122280-MS.

Tongwa P., Baojun B. (2015) A more superior preformed particle gel with potential application for conformance control in mature oilfields, *J. Petrol. Explor. Prod. Technol.* **5**, 201–210. https://doi.org/10.1007/s13202-014-0136-8.

Zhao G., You Q., Tao J., Gu C., Aziz H., Ma L., Dai C. (2018) Preparation and application of a novel phenolic resin dispersed particle gel for in-depth profile control in low permeability reservoirs, *J. Petrol. Sci. Eng.* **161**, 703–714. https://doi.org/10.1016/j.petrol.2017.11.070.